INNOVATIVE MECHANICAL ENGINEERING **ISSN 2812-9229 (Online)**
University of Niš, Faculty of Mechanical Engineering
VOL. 2, NO 1, 2023, PP. 64 –78

Original scientific paper *

NANOFLUID FLOW AND HEAT TRANSFER IN A VERTICAL CHANNEL WITH AN ELECTRIC AND A MOVING MAGNETIC FIELD

Jelena Petrović[1], Milica Nikodijević Đorđević[2], Miloš Kocić[1], Živojin Stamenković[1], Jasmina Bogdanović Jovanović[1], Miloš Jovanović[1]

1 Faculty of Mechanical Engineering, University of Niš

[2] Faculty of Occupational Safety, University of Niš

Abstract. *This paper discusses fully developed flow and heat transfer of a nanofluid in a vertical channel through a porous medium, for which the Darcy model is used. The channel walls are vertical plates at different constant temperatures. The externally applied magnetic field is homogeneous, perpendicular to the channel walls, and moving at constant velocity in the direction of primary nanofluid flow. The external electric field is homogeneous and perpendicular to the vertical longitudinal plane of the channel. Nanofluid velocity and temperature distributions for different values of the introduced physical parameters were determined and shown graphically. The obtained results were analyzed, emphasizing the possibilities of nanofluid flow and heat transfer control.*

Key words: *nanofluid, heat transfer, moving magnetic field, electric field, porous medium*

1. INTRODUCTION

From the engineering, industrial, and biomedical perspective, nanofluid flow and heat transfer in a magnetic environment is considered a new area of research. Extensive research in this area began near the end of the 20th century and the publication of a study by Choi [1]. The research area remains current to date, as evidenced by the publications by Kasaein et al. [2] and Khanafer and Vafai [3]. Both studies provide detailed reviews of simultaneous use of nanofluids and porous media in order to improve heat transfer. Studies by Aaiza et al. [4] and Khan and Alqahtani [5] considered the unsteady magnetohydrodynamic (MHD) flow and heat transfer in a vertical channel through a porous medium with heat radiation. The former focused on impermeable and the latter on permeable channel walls. The former study also discussed three cases of channel wall

*Received: December 05, 2022 / Accepted December 27, 2022
Corresponding author: Jelena Petrović
Institution Faculty of Mechanical Engineering University of Niš, Serbia
E-mail: jelena.nikodijevic.petrovic@masfak.ni.ac.rs

movement. Nikodijević et al. [6] investigated the unsteady MHD flow and heat transfer in a horizontal channel saturated with a porous medium. The channel walls consisted of isothermal permeable parallel plates. The applied magnetic field was homogeneous and inclined in relation to the channel walls. Basic equations were transformed into their dimensionless forms and solved using the perturbation method. Lima et al. [7] performed a numerical analysis of the fully developed steady MHD flow and heat transfer of two immiscible fluids in an inclined channel with parallel plates as channel walls. They analyzed the effects of buoyancy, moving plates, porous layers, the inclined magnetic field, Joule heating and viscous dissipation, and heat generation/absorption. Raj and Rao [8] studied the unsteady electromagnetohydrodynamic (EMHD) flow and heat transfer of two immiscible fluids in a horizontal channel with impermeable plates, influenced by the Hall current and the Coriolis force. Petrović et al. [9] investigated the EMHD flow and heat transfer of two immiscible fluids in a horizontal channel whose fluid regions were saturated with different porous media. The applied magnetic field was inclined in relation to the channel walls. They analyzed the influence of introduced physical parameters on velocity and temperature distributions. Umavathi and Beg [10] explored the reactive flow and heat transfer in a vertical channel saturated with a non-Darcy porous medium. Using the Robin boundary conditions, they analyzed a homogeneous first-order chemical reaction. Makinde and Eegunjobi [11] studied the simultaneous effects of heat radiation, buoyancy force, thermophoresis, and Brownian motion on energy generation during the couple stress nanofluid MHD flow through a vertical permeable channel. They determined that entropy generation can be efficiently minimized by regulating the values of physical parameters. Umavathi and Sheremet [12] investigated mixed convection in three vertical fluid layers, the middle layer filled with a clear fluid and the end layers, saturated with a porous medium, filled with a nanofluid. They used the Darcy model for the porous medium and the perturbation method for solving the basic equations, which were transformed into their dimensionless forms. Manjeet and Sharma [13] analyzed the MHD flow and heat convection of two immiscible fluids in a permeable horizontal channel. The bottom layer contained a nanofluid (H_2O-Ag) and the top layer contained a Newtonian fluid. Using the finite difference method, they determined velocity and temperature profiles, the skin friction coefficient, and the Nusselt number. Roja and Gireesha [14] numerically analyzed the influence of ionic Hall effect on couple stress nanofluid flow through an inclined microchannel subjected to hydraulic slip, convective boundary conditions, heat generation/absorption, and heat radiation. Mehta et al. [15] explored the effects of heat radiation, generation, and absorption on the unsteady mixed convection MHD nanofluid flow in a vertical channel saturated with a porous medium. Water was used as the base fluid and Ag and Al_2O_3 as the nanoparticles. Umavathi and Oztop [16] presented a numerical simulation analyzing the effects of electric and magnetic fields on nanofluid flow and heat transfer in a vertical channel. The left and the right channel wall temperatures were different but constant. Bhaskar and Venteswarlu [17] investigated the effects of heat generation and radiation on the fully developed natural convective MHD flow in a vertical microporous channel. The reference equations of the problem were transformed into their dimensionless forms and solved using the perturbation method. Das et al. [18] studied the influence of the Hall effect on the unsteady MHD flow and heat transfer of a Casson nanofluid (Ag-EG) in a vertical permeable channel, which was saturated with a porous medium according to the Darcy model.

The authors of the present study reviewed many available studies concerning fluid flow and heat transfer and did not find any study that analyzes the influence of a moving magnetic field on fluid flow and heat transfer. The authors believe that such a study could be useful in industry, biomedicine, and other areas of application. Accordingly, this paper investigates the fully developed nanofluid EMHD flow and heat transfer in a vertical channel. The channel walls consist of impermeable, non-conductive, and isothermal parallel plates. The channel is saturated with a Darcian porous medium. The externally applied electric field is homogeneous and perpendicular to the primary flow direction and the longitudinal plane of the channel. The externally applied magnetic field is homogeneous, perpendicular to the channel walls, and moving at constant velocity in the direction of the primary flow. Special attention is given to the use of the introduced electromagnetic parameters and magnetic field movement for managing nanofluid flow and heat transfer in a vertical channel saturated with a porous medium.

2. MATHEMATICAL FORMULATION

This paper focuses on a fully developed nanofluid EMHD flow and heat transfer in a vertical channel, whose physical configuration with the selected coordinate system is shown in Figure 1. The channel walls are impermeable and non-conductive vertical parallel plates at distance h from each other. The left channel wall is at constant temperature T_{w2}, and the right at T_{w1} ($T_{w1}>T_{w2}$). The external homogeneous magnetic field has induction B along the direction of the y-axis, and it moves at constant velocity u_0 in the direction of the x-axis. The external homogeneous electric field E follows the direction of the z-axis. The nanofluid flows at velocity u in the direction of the x-axis under the influence of buoyancy force and constant pressure gradient $P_1=-\partial p/\partial x$. The channel is saturated with a Darcian porous medium of permeability K_0. The fluid temperature in the channel is T.

Momentum and energy equations and boundary conditions that describe this flow and heat transfer have the following forms, respectively [12], [19]:

$$\begin{gathered} P_1 + \mu_{nf}\frac{d^2u}{dy^2} - \frac{\mu_{nf}}{K_0}u - B\sigma_{nf}[E + (u-u_0)B] = g(\rho\beta)_{nf}(T - T_{w2}) = 0 \\ k_{nf}\frac{d^2T}{dy^2} + \mu_{nf}\left(\frac{du}{dy}\right)^2 + \frac{\mu_{nf}}{K_0}u^2 + \sigma_{nf}[E + (u-u_0)B]^2 = 0 \\ u(0) = 0, u(h) = 0, T(0) = T_{w2}, T(h) = T_{w1}. \end{gathered} \tag{1}$$

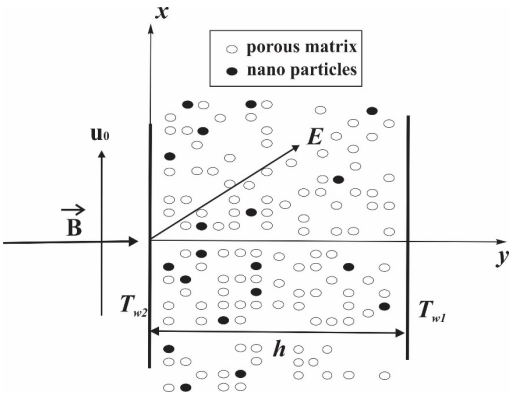

Fig. 1 Physical configuration

Nanofluid properties, namely density, dynamic viscosity, coefficient of thermal expansion, electroconductivity, and thermal conductivity are given in the following classical expressions [18]:

$$\rho_{nf} = a_1\rho_f, \mu_{nf} = m^{-1}\mu_f, (\rho\beta)_{nf} = a_2(\rho\beta)_f$$
$$\sigma_{nf} = \varphi_1\sigma_f, k_{nf} = \varphi_2 k_f, a_1 = \Psi(1,\rho), a_2 = \Psi(\rho,\beta)$$
$$m = (1-\phi)^{2.5}, \varphi_1 = X(\sigma), \varphi_2 = X(k), \tag{2}$$
$$\psi(\zeta,\eta) = 1 - \phi + \phi\frac{(\zeta,\eta)_s}{(\zeta,\eta)_f}$$
$$\mathrm{X}(X) = \frac{2(1-\phi)X_f + (1+2\phi)X_s}{(2+\phi)X_f + (1-\phi)X_s}$$

where subscripts *f*, *s*, and *nf* denote the base fluid, the nanoparticles, and the nanofluid, respectively, while ϕ denotes the volume fraction of the nanoparticles.

Before system of equations (1) is solved, it needs to be transformed into its dimensionless form. To that end, dimensionless quantities are introduced by the following expressions:

$$y^* = \frac{y}{h}, u^* = \frac{u}{U}, \theta = \frac{T - T_{w2}}{T_{w1} - T_{w2}} \tag{3}$$

where U is the characteristic velocity to be selected later in the paper. Using dimensionless quantities (3), system of equations (1) is transformed into the following dimensionless system of equations with the corresponding dimensionless boundary conditions:

$$\frac{d^2u}{dy^2} - \omega^2 u + aM\theta = R_1$$
$$\frac{d^2\theta}{dy^2} + \frac{Br}{m\varphi_2}\left[\left(\frac{du}{dy}\right)^2 + \omega u^2 + 2Ru + R_2\right] = 0, \tag{4}$$
$$u(0) = 0, u(1) = 0, \theta(0) = 0, \theta(1) = 1,$$

where the asterisk symbol * is omitted for the sake of brevity, but it is hereinafter implied that the quantities are dimensionless, with the following notation:

$$a = ma_2, P = P_1 \frac{h^2}{U\mu_f}, M = g\frac{(\rho\beta)_f h^2}{U\mu_f}(T_{w1} - T_{w2})$$

$$\omega^2 = \Lambda + m\varphi_1 Ha^2, d = \frac{u_0}{U}, R = m\varphi_1 Ha^2(K - d),$$

$$R_1 = R - mP, R_2 = R(K - d), \Lambda = \frac{h^2}{K_0}, K = \frac{E}{BU}, \tag{5}$$

$$Ha = Bh\sqrt{\frac{\sigma_f}{\mu_f}}, Br = \frac{\mu_f}{k_f}\frac{U^2}{T_{w1} - T_{w2}}.$$

where Λ – porosity factor, K – external power factor, Ha – Hartmann number, Br – Brinkman number, and d – dimensionless velocity of the magnetic field.

3. SOLUTIONS

The next step is to solve system of equations (4), for which the perturbation method is used. Accordingly, velocity and temperature solutions are assumed to have the following representations:

$$(u, \theta) = (u_0, \theta_0) + Br(u_1, \theta_1) + \cdots \tag{6}$$

where the Brinkman number is taken as the perturbation parameter, because, as previous research has shown, its value is low in the majority of practical problems.

By substituting representations (6) in system of equations and boundary conditions (4) and by separating the expressions next to the zeroth and first degree of the Brinkmann number, the zeroth order system of equations and zeroth order boundary conditions are expressed as follows:

$$\frac{d^2u_0}{dy^2} - \omega^2 + aM\theta_0 = R_1, \frac{d^2\theta_0}{dy^2} = 0,$$

$$u_0(0) = 0, u_0(1) = 0, \theta_0(0) = 0, \theta_0(1) = 1. \tag{7}$$

The first order system of equations and the first order boundary conditions have the following forms:

$$\frac{d^2u_1}{dy^2} - \omega^2 u_1 + aM\theta_1 = 0,$$

$$\frac{d^2\theta_1}{dy^2} + \frac{1}{m\varphi_2}\left[\left(\frac{du_0}{dy}\right)^2 + \omega u_0^2 + 2Ru_0 + R_2\right] = 0, \tag{8}$$

$$u_1(0) = 0, u_1(1) = 0, \theta_1(0) = 0, \theta_1(1) = 0.$$

First, system (7) is solved using the usual procedure for solving regular differential equations, resulting in the following representations:

$$\theta_0(y) = y,$$

$$u_0(y) = D_1 exp(\omega y) + D_2 exp(-\omega y) + \frac{aM}{\omega^2} y - \frac{R_1}{\omega^2}. \quad (9)$$

Finally, system (8) is solved, resulting in the following representations:

$$\theta_1(y) = -\frac{1}{m\varphi_2}\left[\frac{1}{2}D_1^2 exp(2\omega y) + \frac{1}{2}D_2^2 exp(-2\omega y) + (R_3 + R_4 y)exp(\omega y) + (R_5 + R_6 y)exp(-\omega y) + R_7 y^4 + R_8 y^3 + R_9 y^2 + C_3 y + C_4\right]$$

$$u_1(y) = (D_3 + R_{12} y + R_{13} y^2)exp(\omega y) + (D_4 + R_{14} y + R_{15} y^2)exp(-\omega y) + R_{10} exp(2\omega y) + R_{11} exp(-2\omega y) + R_{16} y^4 + R_{17} y^3 + R_{18} y^2 + R_{19} y + R_{20}. \quad (10)$$

where the integration constants are expressed as:

$$C_3 = \frac{1}{2}(D_1^2 + D_2^2) + R_3 + R_5 - \frac{1}{2}D_1^2 exp(2\omega) - \frac{1}{2}D_2^2 exp(-2\omega) - (R_3 + R_4)exp(\omega) - (R_5 + R_6)exp(-\omega) - R_7 - R_8 - R_9,\ D_4 = R_{21} - D_3. \quad (11)$$

and the following notation is used for brevity:

$$R_3 = \frac{2D_1}{\omega^2}\left(R - R_1 - \frac{aM}{\omega}\right), R_4 = \frac{2MaD_1}{\omega^2}$$

$$R_5 = \frac{2D_2}{\omega^2}\left(R - R_1 + \frac{aM}{\omega}\right), R_7 = \frac{1}{12}\frac{a^2M^2}{\omega^2},$$

$$R_8 = \frac{1}{3}\frac{aM}{\omega^2}(R - R_1), R_{10} = \frac{1}{6}\frac{SD_1^2}{\omega^2}, R_{11} = \frac{1}{6}\frac{SD_2^2}{\omega^2},$$

$$R_9 = \frac{1}{2}\left(\frac{a^2M^2}{\omega^4} + \frac{R_1^2}{\omega^2} - \frac{2RR_1}{\omega^2} + R_2\right), R_6 = \frac{2MaD_2}{\omega^2},$$

$$R_{13} = \frac{1}{4}S\frac{R_4}{\omega}, R_{14} = -\frac{1}{4}S\frac{2\omega R_5 + R_6}{\omega^2}, S = \frac{aM}{m\varphi_2}, \quad (12)$$

$$R_{16} = -S\frac{R_7}{\omega^2}, R_{17} = -S\frac{R_8}{\omega^2}, R_{18} = -S\frac{12R_7 + \omega^2 R_9}{\omega^4}$$

$$R_{19} = -S\frac{6R_8 + \omega^2 C_3}{\omega^4}, R_{12} = S\frac{2\omega R_3 - R_4}{4\omega^2},$$

$$R_{21} = -R_{10} - R_{11} - R_{20}, R_{15} = -\frac{1}{4}S\frac{R_6}{\omega},$$

$$R_{20} = -S\frac{24R_7 + 2\omega^2 R_9 + \omega^4 C_4}{\omega^6}$$

$$R_{22} = -R_{10} exp(2\omega) - R_1 exp(-2\omega) - (R_{12} + R_{13})exp(\omega) - (R_{14} + R_{15})exp(-\omega) - R_{16} - R_{17} - R_{18} - R_{19} - R_{20}.$$

4. RESULTS AND ANALYSIS

The previous section determined the analytical explicit expressions for the nanofluid flow velocity and temperature distribution in the channel. These expressions also depend on the introduced physical parameters that are characteristic of the analyzed problem. To determine the effect of the parameters on the distributions, this section presents the results in the case of the water-copper nanofluid. Characteristic velocity was selected such that quantity M is the Grashof number (Gr). The applied values of water-copper

physical properties are given in Table 1. For simpler and clearer analysis, the velocity and temperature distributions are presented graphically in the figures below.

Table 1 Physical properties

Physical properties	ρ (kg/m3)	k (W/(Km))	σ (S/m)	μ (Pas)	β(1/k)
H_20	997.1	0.613	$5.5 \cdot 10^{-6}$	0.001	4179
Cu	8933	401	$59.6 \cdot 10^{6}$	-	385

Figs. 2 and 3 show velocity and temperature distributions, respectively, for the water-copper nanofluid and for different Hartmann numbers. According to Fig. 2, higher Hartmann numbers increase nanofluid velocities in the channel and the shear stress on the channel walls. A flattening of the velocity profile is also observed. The increase in velocity is due to the increased Lorentz force, which in this case acts as the active force. Fig. 3 shows that higher Hartmann numbers increase nanofluid temperatures in the channel. For Ha=2.5, temperature distribution is the closest to the distribution of conductive heat transfer. For Ha=2.5 and Ha=5, heat is transferred from the right wall to the nanofluid, whereas for Ha=10, heat is transferred from the nanofluid to the wall.

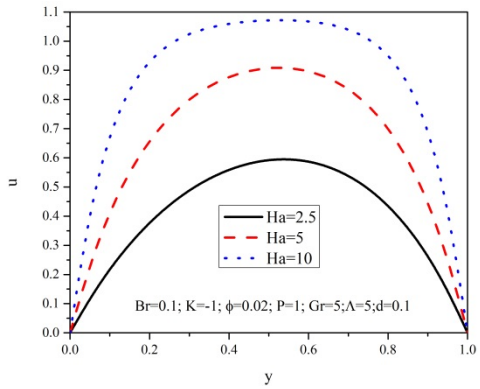

Fig. 2 Velocity distributions for different Ha values

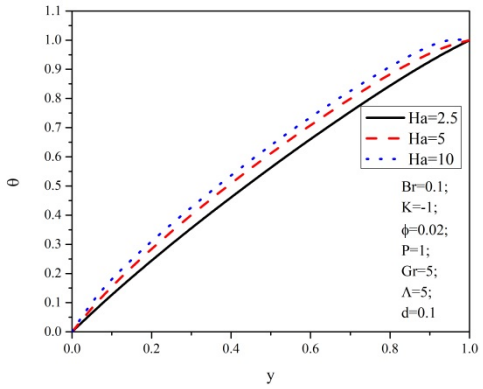

Fig. 3 Temperature distributions for different Ha values

Figs. 4 and 5 show velocity and temperature distributions for different porosity factors, respectively. Fig. 4 shows that higher porosity factors reduce nanofluid velocity in the channel, reduce shear stress on the channel walls, and flatten the velocity profile. This is due to the higher intensity of the porous matrix resistance force in the channel. Fig. 5 shows that higher porosity factors correspond to higher nanofluid temperatures. For all temperature distributions shown in the figure, heat is transferred from the right wall to the nanofluid. The temperature increases because the energy to overcome the fluid flow resistance force in the porous matrix increases and is transformed into thermal energy.

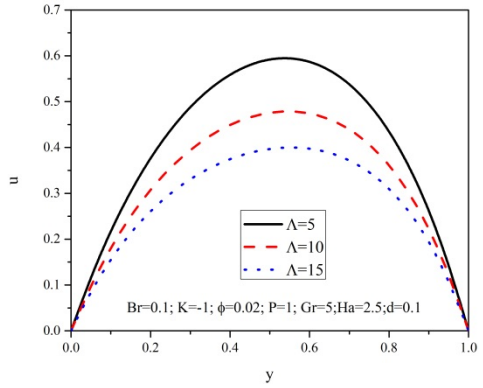

Fig. 4. Velocity distributions for different Λ values

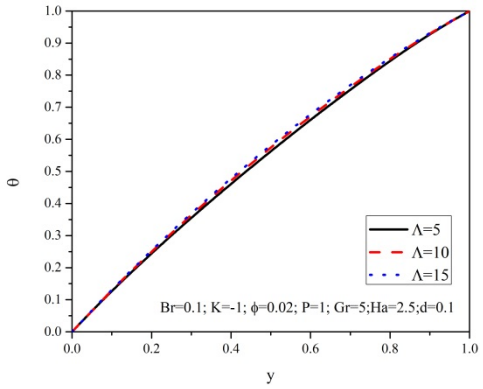

Fig. 5 Temperature distributions for different Λ values

Figs. 6 and 7 show velocity and temperature distributions for different nanoparticle volume fractions, respectively. The figures indicate that that the increase in nanoparticle volume fraction, i.e., increased concentration of solid substance in the fluid, reduces the nanofluid's flow velocity and temperature.

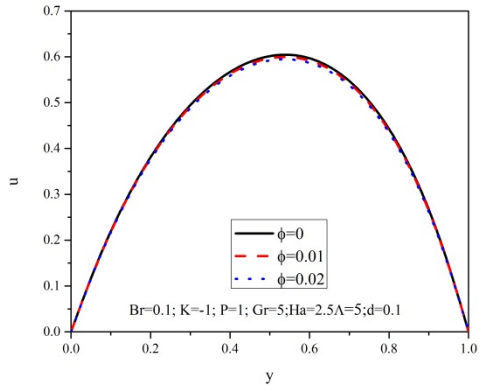

Fig. 6 Velocity distributions for different ϕ values

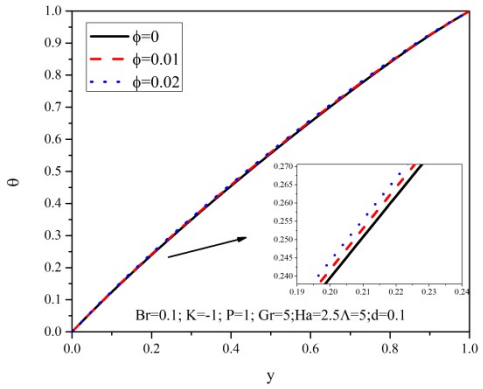

Fig. 7 Temperature distributions for different ϕ values

Figs. 8 and 9 show velocity and temperature distributions for different Brinkman numbers, respectively. It is apparent that the increase in the Brinkman number increases the nanofluid velocity and temperature. Higher Brinkman numbers correspond to lower temperature differences between the channel walls, which in turn increases nanofluid temperatures. The increase in nanofluid temperature then increases the intensity of the buoyancy force, which accelerates the nanofluid flow. For all temperature distributions shown in Fig. 9, heat is transferred from the right wall to the nanofluid.

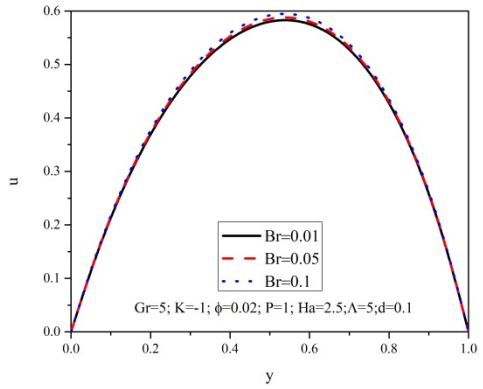

Fig. 8 Velocity distributions for different Br values

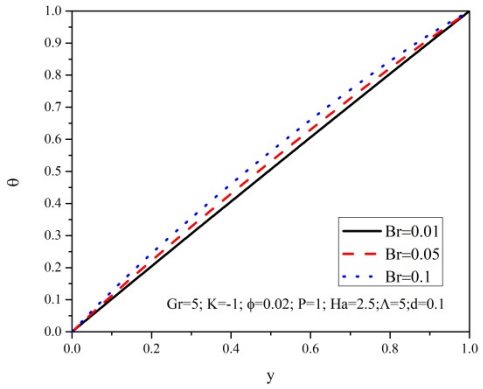

Fig. 9 Temperature distributions for different Br values

Figs. 10 and 11 show velocity and temperature distributions for different external magnetic field dimensionless velocities, respectively. Higher velocities of the external magnetic field increase nanofluid velocities and temperatures. In this case, higher magnetic field velocity increases the intensity of the Lorentz force, which in turn accelerates the nanofluid flow. At the same time, it increases Joule heating, which increases the nanofluid temperature. For all temperature distributions shown in Fig. 11, heat is transferred from the right channel wall to the nanofluid.

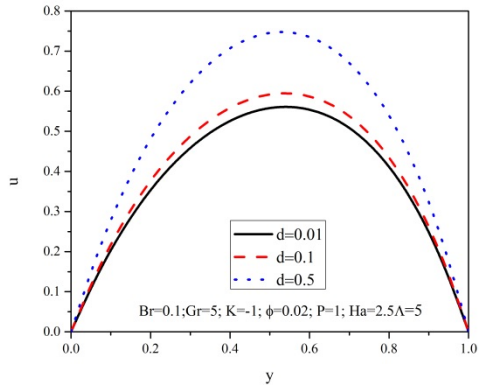

Fig. 10 Velocity distributions for different d values

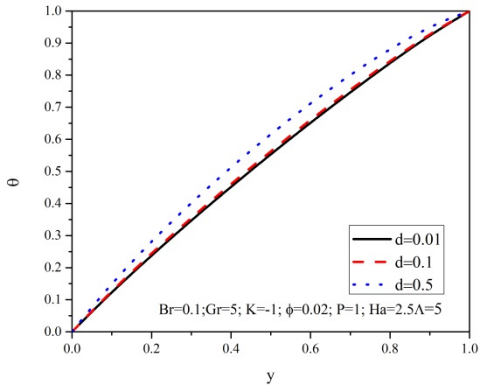

Fig. 11 Temperature distributions for different d values

Figs. 12 and 13 show velocity and temperature distributions for different external power factors, respectively. Evidently, changing the K values will also change the nanofluid flow velocity magnitude and direction. For K=0, heat transfer in the channel is usually conductive, while the heat is transferred from the right wall to the nanofluid for all three temperature profiles. Temperature distributions for K=±1 differ only slightly.

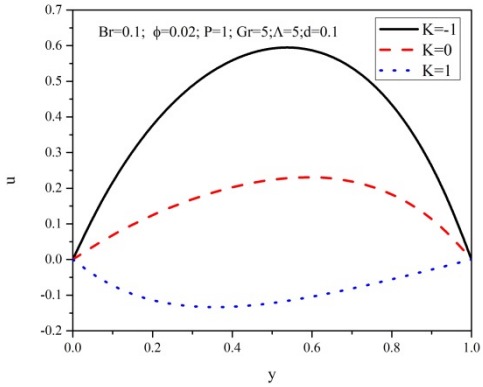

Fig. 12 Velocity distributions for different K values

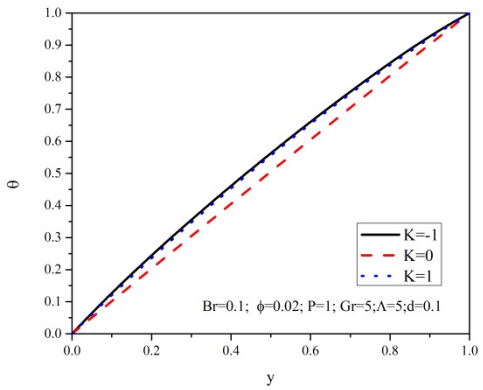

Fig. 13 Temperature distributions for different K values

Figs. 14 and 15 show velocity and temperature distributions for different Grashof numbers, respectively. Analysis of velocity distributions in Fig. 14 indicates that higher Grashof numbers correspond to higher nanofluid velocities and higher shear stresses on the channel walls. Velocity is increased by the increase in buoyancy force intensity. Fig. 15 shows that the temperature distributions differ only slightly and that heat is transferred from the right wall to the nanofluid in all three cases.

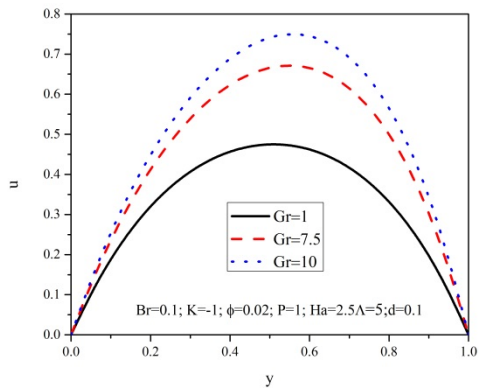

Fig. 14. Velocity distributions for different Gr values

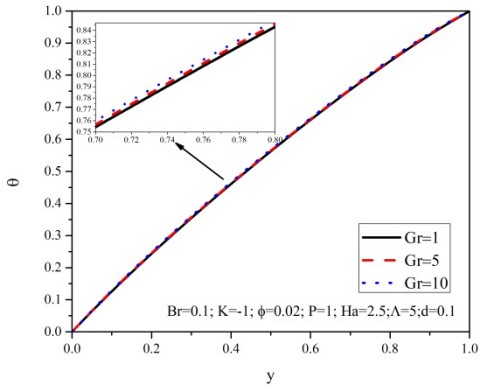

Fig. 15 Temperature distributions for different Gr values

5. CONCLUSION

This paper discussed the flow and heat transfer of a nanofluid in the channel consisting of two parallel vertical plates. The channel was saturated with a porous medium and the plates were at different constant temperatures. The nanofluid was influenced by an external electric field and an external moving magnetic field. Analytical expressions were determined for nanofluid velocity and temperature distributions in relation to multiple introduced physical parameters. A portion of the obtained results were presented graphically and the effects of the introduced physical parameters on the nanofluid flow and heat transfer were analyzed.

According to the results, it was concluded that a higher Hartmann number increases the nanofluid's flow velocity as well as its temperature. Higher porosity factor decreases the nanofluid's velocity but increases its temperature. Higher nanoparticle volume fraction decreases both the velocity and the temperature of the nanofluid. A higher Grashof number increases the flow velocity and only slightly affects temperature distribution. A higher Brinkman number increases nanofluid velocity as well as temperature. Higher external magnetic field velocity increases both the velocity and the temperature of the nanofluid. Finally, changes in the external power factor will also change the nanofluid's flow velocity magnitude as well as its direction and temperature. This indicates that each of the introduced physical parameters can be used to manage nanofluid MHD flow and heat transfer in a vertical channel.

Acknowledgment: *This research was financially supported by the Ministry of Education, Science and Technological Development of the Republic of Serbia.*

REFERENCES

1. Choi, S.U.S, 1995, *Enhancing thermal conductivity of fluids with nanoparticles*, ASME Int. Mech. Eng., 69, 99-105.

2. Alibakhsh Kasaein, Reza Daneshazarian, Omid Mahian, Liona Kolesi, Ali J. Chamkha, 2017, Somchai Wongwises, Ioan Pop, *Nanofluid flow and heat transfer in porous media: A review of the latest developments,* International Journal of Heat and Mass Transfer 107, pp. 778-791.
3. Khalil Khanafer, Kambiz Vafai, 2018, *Applications of nanofluids in porous medium, A critical review*, Journal of Thermal Analysis and Calorimetry, Vol. 135, Issue 2, pp. 1479-1492.
4. Gul Aaiza, Ilyas Khan and Sharidan Shafie, 2015, *Energy Transfer in Mixed Convection MHD Flow of Nanofluid Containing Different Shapes of Nanoparticles in a Channel Filled with Saturated Porous Medium,* Nanoscale Research Letters 10:490.
5. Ilyas Khan and Aisha M. Alqahtani, 2019, *MHD Nanofluids in a Permeable Channel with Porosity,* Symmetry, 11, 378.
6. Nikodijević M., Stamenković Ž., Petrović J., Kocić M., 2020, *Unsteady fluid flow and heat transfer through a porous medium in a horizontal channel with an inclined magnetic field*, Transactions of Famena, International Scientific Journal, University of Zagreb, Faculty of Mechanical Engineering and Naval Architecture, Vol.44, No.4, pp.31–46.
7. J.A. Lima, G.E. Assad and H.S. Pavia, 2016, *A simple approach to analyze the fully developed two-phase magnetoconvection type flows in inclined parallel-plate channels*, Latin American Applied Research, 46(3), pp. 93-98.
8. T. Linga Raju and B. Venkat Rao, 2022, *Unsteady electro-magneto hydrodynamic flow and heat transfer of two ionized fluids in a rotating system with hall currents*, Int. J. of Applied Mechanics and Engineering, Vol. 27, No. 1; pp. 125-145.
9. Jelena D. Petrović, Živojin M. Stamenković, Miloš M. Kocić, Milica D. Nikodijević, 2016, *"Porous medium magnetohydrodynamic flow and heat transfer of two immiscible fluids",* Thermal Science, Vol. 20, Suppl. 5 pp. S1405 - S1417.
10. J.C. Umavathi, O. Anwar Beg, 2019, *Numerical study of double-diffusive dissipative reactive convective flow in an open vertical duet containing a non-Darcy porous medium with Robin boundary conditions*, Journal of Engineering Mathematics 119(1).
11. Oluwole Daniel MAKINDE and Adetayo Samuel EEGUJOBI, 2017, *MHD couple stress nanofluid flow in a permeable wall channel with entropy generation and nonlinear radiative heat*, Journal of Thermal Science and Technology, Vol. 12, No. 2.
12. Umavathi J. C., Sheremet M. A, 2020, *Heat transfer of viscous fluid in a vertical channel sandwiched between nanofluid porous zones*, Journal of Thermal Analysis and Calorimetry 144(4).
13. Manjeet and Mukesh Kumar Sharma, 2020, *MHD flow and heat convection in a channel filled with two immiscible Newtonian and nanofluid fluids*, JP Journal of Heat and Mass Transfer, Vol. 21, No. 1, pp. 1-21.
14. A. Roja, B.J. Gireesha, 2020, *Impact of Hall and Ion effects on MHD couple stress nanofluid flow through an inclined channel subjected to convective, hydraulic slip, heat generation and thermal radiation*, Heat Transfer, Vol. 49, Issue 6, pp. 3314-3333.
15. R. Mehta, V. S. Chouhan and T. Mehta, 2020, *MHD flow of nanofluids in the presence of porous media, radiation and heat generation through a vertical channel*, Journal of Physics: Conference Series 1504, 012008.
16. J.C. Umavathi and Hakan F. Oztop 2021, *Investigation of MHD and applied electric field effects in a conduit crammed with nanofluids*, International Communications in Heat and Mass Transfer, Vol. 121:105097.
17. Ponna Bhaskar and Malapati Venteswarlu 2021, *Influence of Heat Generation and Thermal Radiation on MHD Flow in a Vertical Micro-Porous_Chanel in the Presence of Viscous Dissipation*, Mapana – Journal of Sciences, Vol. 20, No. 2, pp. 27-58.
18. Das S., Banu A: S., Jana R.N., Makine O.D. 2022, *Hall Current's Impact on Ionized Ethylene Glycol Containing Metal Nanoparticles Flowing Through Vertical Permeable Channel*, Journal of Nanofluids, Vol. 11, No. 3, pp. 453-467(15).
19. I.M. Kirko, G.E. Kirko 2009, *Magnetic hydrodynamics, Contemporary view of the problem;* Computer Research Institute; Moscow, Izhevsk, 632 pages.